Journal of Theoretical and Applied Information Technology
31st March 2013. Vol. 49 No.3

ISSN: 1992-8645 www.jatit.org E-ISSN: 1817-3195

A MODIFIED EKF ALGORITHM FOR GPS POINT DYNAMIC POSITIONING AND VELOCITY MEASUREMENT

[1,2] SONG DAN, [1,3] ZHANG PENGFEI, [1,4] XU CHENGDONG
[1] School of Aerospace Engineering, Beijing Institute of Technology, Beijing, 100081, China.
E-mail: [2]songdan0207@163.com, [3] successful.2008@163.com ,[4]xucd@bit.edu.cn

ABSTRACT

Extended Kalman Filter (EKF) algorithm is widely used in GPS positioning and velocity measurement. As for EKF algorithm, the approximate initial position of the receiver is indispensable; otherwise the time consumption of the first positioning is too high because of the filter's low convergence rate. A modified EKF algorithm named delayed update EKF (DU-EKF) algorithm for GPS point dynamic positioning and velocity measurement is proposed in this paper, which can speed up the convergence rate of the filter without the receiver's approximate initial position. Furthermore, it can improve the accuracy of positioning and velocity measurement. Three kinds of algorithms are used in the simulation of this paper to compare with the modified EKF algorithm: iterative least square (ILS) algorithm, EKF algorithm with the Zero initial state vector (ZEKF) and EKF algorithm with the initial state vector which is Close to the actual situation (CEKF).

Keywords: *Extended Kalman Filter (EKF), GPS, Positioning, Velocity measurement*

1. INTRODUCTION

GPS point dynamic positioning and velocity measurement, with its excellence of only requiring a single frequency receiver, is widely used in vehicle navigation, marine positioning and field exploration for its low cost and high efficiency [1, 2]. Least Square (LS) algorithm [2] and Extended Kalman Filter (EKF) algorithm [3, 4] are commonly used for GPS point dynamic positioning and velocity measurement. As for LS algorithm, the approximate initial position of the receiver is indispensable because the pseudorange equation which depicts the range between the receiver and visible satellites should be linearized by Taylor series. To avoid searching for the approximate initial position and to achieve higher accuracy, modified algorithms based on LS have been proposed, such as weighted least square (WLS) algorithm [5] and iterative least square (ILS) algorithm [6]. Both of them can be used to position and measure velocity without the receiver's approximate initial position, and thus higher accuracy can be obtained than that of LS algorithm. However, the accuracy is much lower than that of EKF algorithm [5, 7], just because LS algorithm only utilizes observation data belonging to the current epoch while EKF algorithm utilizes observation data of previous epochs as well [8]. As for EKF algorithm, the pseudorange equation and the Doppler shift equation should also be linearized. Consequently, if the initial state vector deviates too much from the actual situation, convergence rate of filter will be very slow. In other words, it will take long time for the first positioning. Therefore, EKF algorithm also needs the approximate initial position of the receiver.

A modified EKF algorithm is proposed in this paper to position and measure velocity without the approximate initial position of the receiver, namely delayed update EKF (DU-EKF) algorithm in which the state error covariance matrix begins to be updated after several calculating epochs. This algorithm ensures a fast convergence rate and keeps the superior accuracy which EKF algorithm owns. To compare with the modified EKF algorithm, three kinds of algorithms are used in simulation of this paper. They are ILS algorithm, EKF algorithm with the Zero initial state vector (ZEKF) and EKF algorithm with the initial state vector which is Close to the actual situation (CEKF) respectively.

The paper is organized as follows: Section 2 provides a description of EKF algorithm for GPS point dynamic positioning and velocity measurement. Section 3 introduces the modified EKF algorithm namely DU-EKF algorithm. Section 4 shows the performance of DU-EKF algorithm by simulation. In the simulation, the Singer model [9] is selected to describe the receiver's uniform

Journal of Theoretical and Applied Information Technology
31st March 2013. Vol. 49 No.3

ISSN: 1992-8645 www.jatit.org E-ISSN: 1817-3195

motion. And Section 5 presents conclusions.

2. DESCRIPTION OF EKF ALGORITHM FOR GPS POINT DYNAMIC POSITIONING AND VELOCITY MEASUREMENT

For GPS point dynamic positioning and velocity measurement, two kinds of models are used in EKF. One is the dynamic model describing the relationship of the receiver's state vectors belonging to two adjacent epochs respectively, and the other is the observation model depicting the relationship between the observation vector and the receiver's state vector. EKF requests to linearize the models which are nonlinear by Taylor series.

In terms of GPS point dynamic positioning and velocity measurement, the dynamic model can be CV model [10], CA model [11] or Singer model [9] which is linear while the observation model are both pseudorange model and Doppler shift model which are nonlinear. The basic EKF equations are as follows [9]:

State transition equation:

$$\boldsymbol{X}_k = \boldsymbol{\Phi}_{k|k-1}\boldsymbol{X}_{k-1} + \boldsymbol{\Gamma}_{k|k-1}\boldsymbol{\omega}_{k-1} \quad (1)$$

Observation equation:

$$\boldsymbol{Z}_k = f_k(\boldsymbol{X}_k) + \boldsymbol{v}_k \quad (2)$$

State transition equation and observation equation correspond to dynamic model and observation model respectively. Formula (2) should be linearized to Formula (3):

$$\Delta\boldsymbol{Z}_k = H_k \Delta\boldsymbol{X}_k + \boldsymbol{v}_k \quad (3)$$

In Formula (1)-(3), k denotes epoch number; $\boldsymbol{X}_k$ is the state vector at *kth* epoch, which incorporates all the receiver's motion state parameters needed to be solved; $\boldsymbol{\Phi}_{k|k-1}$ is the state transition matrix; $\boldsymbol{\omega}_{k-1}$ is vector of dynamic model noise; $\boldsymbol{\Gamma}_{k|k-1}$ is the noise driven matrix; $\boldsymbol{v}_k$ is vector of observation noise; H_k is the Jacobian matrix of $f_k(\cdot)$,namely observation matrix; $\Delta\boldsymbol{X}_k = \boldsymbol{X}_k - \boldsymbol{X}_{k-1}$; $\Delta\boldsymbol{Z}_k = \boldsymbol{Z}_k - \boldsymbol{Z}_{k-1}$; $\boldsymbol{Z}_{k-1} = f_{k-1}(\boldsymbol{X}_{k-1})$.

The steps of EKF algorithm for GPS point positioning and velocity measurement are as follows (Q_{k-1} and O_k are covariance matrices of $\boldsymbol{\Gamma}_{k|k-1}\cdot\boldsymbol{\omega}_{k-1}$ and $\boldsymbol{v}_k$):

1. Reckon the predictive state vector $\hat{\boldsymbol{X}}_{k|k-1}$ of $\boldsymbol{X}_k$:

$$\hat{\boldsymbol{X}}_{k|k-1} = \boldsymbol{\Phi}_{k|k-1}\hat{\boldsymbol{X}}_{k-1} \quad (4)$$

   Where $\hat{\boldsymbol{X}}_{k-1}$ is the optimal estimation of filtering for $\boldsymbol{X}_{k-1}$.

2. Reckon $P_{k|k-1}$ which is the error covariance matrix of $\hat{\boldsymbol{X}}_{k|k-1}$:

$$P_{k|k-1} = \boldsymbol{\Phi}_{k|k-1}P_{k-1}\boldsymbol{\Phi}_{k|k-1}^T + Q_{k-1} \quad (5)$$

3. Calculate the Kalman gain matrix K_k :

$$K_k = P_{k|k-1}H_k^T[H_k P_{k|k-1} H_k^T + O_k]^{-1} \quad (6)$$

4. Get the optimal filtering estimation $\hat{\boldsymbol{X}}_k$ of $\boldsymbol{X}_k$:

$$\hat{\boldsymbol{X}}_k = \hat{\boldsymbol{X}}_{k|k-1} + K_k \Delta\boldsymbol{Z}_k \quad (7)$$

   Where $\hat{\boldsymbol{X}}_k$ can be considered as the calculation result at *kth* epoch.

5. Get the error covariance matrix P_k of $\hat{\boldsymbol{X}}_k$:

$$P_k = [I - K_k H_k]P_{k|k-1} \quad (8)$$

The process for EKF algorithm at *kth* epoch can be seen in *Figure 1* [8].

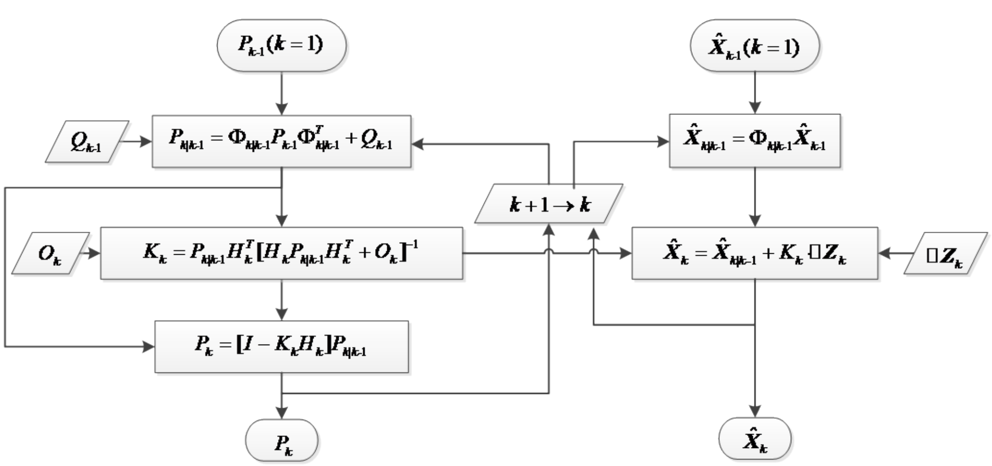

Figure 1: Caculating steps of EKF at kth epoch

ISSN: 1992-8645 www.jatit.org E-ISSN: 1817-3195

3. DELAYED UPDATE EKF (DU-EKF) ALGORITHM FOR GPS POINT DYNAMIC POSITIONING AND VELOCITY MEASUREMENT

When using EKF algorithm for GPS point dynamic positioning, assigning $\boldsymbol{0}$ to $\hat{X}_0$ and a diagonal matrix with large positive elements to P_0 is an easy way of driving filter. However, as a result of the big difference between the zero vector and the actual X_0, the slow convergence rate of filter elongates the time of first positioning [8]. Assigning a vector which is close to the actual X_0 to $\hat{X}_0$ can accelerate the convergence rate of filter [3], nevertheless, it's hard to define how close $\hat{X}_0$ is to X_0 can make the filter converge fast. In addition, it is impossible to obtain the receiver's approximate initial position all the time.

As seen in *Figure 1*, in EKF algorithm, the optimal filtering estimation of the state vector $\hat{X}_k$ and its error covariance matrix P_k are updated simultaneously at each epoch [1]. After a large number of experiments, one regulation is found which can accelerate convergence of filter and achieve higher accuracy. When using EKF algorithm for GPS positioning and velocity measurement, $\hat{X}_0$ is still assigned to $\boldsymbol{0}$ and its error covariance matrix P_0 to diagonal matrix with large positive elements. However, only $\hat{X}_k$ is updated at each epoch, while P_k begins to be updated after *mth* epoch ($2<m<6$). In other words, only $\hat{X}_k$ is updated when $k\le m$ while $\hat{X}_k$ and P_k are both updated when $k>m$. Therefore a modified EKF algorithm, named DU-EKF algorithm, is proposed to utilize this regulation. The process of DU-EKF algorithm is shown in *Figure 2*, specific example of $m=3$ is as follows:

At 1^{st} epoch, input $\hat{X}_0$ and P_0, reckon $\hat{X}_{1|0}$, $P_{1|0}$, K_1 and $\hat{X}_1$, $k=1\le 3$, $P_1=P_0$;
At 2^{nd} epoch, input $\hat{X}_1$ and P_1, reckon $\hat{X}_{2|1}$, $P_{2|1}$, K_2 and $\hat{X}_2$, $k=2\le 3$, $P_2=P_0$;
At 3^{rd} epoch, input $\hat{X}_2$ and P_2, reckon $\hat{X}_{3|2}$, $P_{3|2}$, K_3 and $\hat{X}_3$, $k=3\le 3$, $P_3=P_0$;
At 4^{th} epoch, input $\hat{X}_3$ and P_3, reckon $\hat{X}_{4|3}$, $P_{4|3}$, K_4 and $\hat{X}_4$, $k=4>3$, $P_4=[I-K_4H_4]P_{4|3}$;
⋮
(Same as at *4th* epoch)

After a lot of experiments, it is found that: if $m\le 2$, the convergence rate of filter can't be improved. If $2<m<6$, it takes only 5 epochs for the optimal estimation of filtering to approach the true value; from *10th* epoch to *15th* epoch, the precision of optimal filtering estimation can be the same as that of CEKF algorithm; after *15th* epoch, the precision will be improved gradually and slightly. But if $m\ge 6$, the optimal estimation of filtering will not converge to the true value until a dozen of epochs. In other words, the convergence rate of $m\ge 6$ is much slower than that of $2<m<6$. That's why the range of *m* is from 2 to 6 in DU-EKF algorithm.

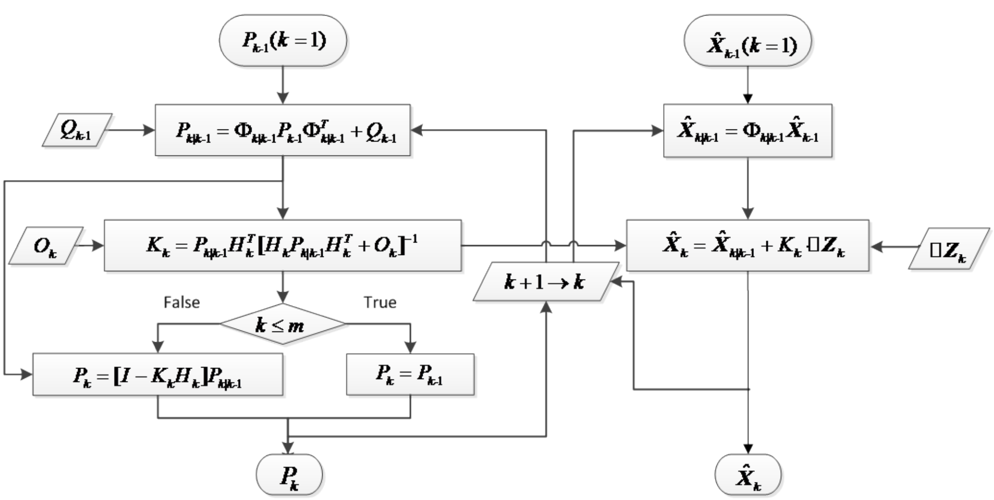

Figure 2: Caculating steps of DU-EKF at kth epoch

ISSN: 1992-8645 www.jatit.org E-ISSN: 1817-3195

4. SIMULATION

During the simulation of GPS point dynamic positioning and velocity measurement, pseudorange and Doppler shift are obtained from a simulator which produces pseudorange and Doppler data with Gauss white noise. The standard deviation of Gauss white noise for pseudorange and Doppler shift is 8m and 0.2m/s respectively. Moreover, the requirement of EKF algorithm that the initial conditions of the state of system and the priori statistical characteristics of error model should be zero mean white noise with known variances [1, 8] respectively is contented. Simultaneously, the simulation environment is close to the actual situation.

In the simulation, the receiver's actual position is $[5^\circ, 5^\circ, 0m]$ in geodetic coordinate system while $[6329853.79, 553790.45, 552184.40]\ m$ in Earth Centered Earth Fixed coordinate (ECEF) [12].The receiver is assumed to do uniform motion with a velocity of $[5,5,5]$ m/s in ECEF. The initial simulation time is 2011-6-20 2:00:00 in UTC [13]. The simulation step is 1*s*, which means the interval between two adjacent epochs.

ILS algorithm, ZEKF algorithm and CEKF algorithm are all used to compare with DU-EKF algorithm. In ZEKF algorithm, CEKF algorithm and DU-EKF algorithm, the Singer model [8] is chosen as the dynamic model and the quartz clock [7] is chosen as the clock model. The clock model is considered as the dynamic model of clock. Both the pseudorange and Doppler shift equations are chosen as observation model. The parameters of EKF based on these models are explained as follows:

1. $\boldsymbol{X}_k$ and P_k

$$\boldsymbol{X}_k = [x_k^u, v_k^{ux}, a_k^{ux}, y_k^u, v_k^{uy}, a_k^{uy}, z_k^u, v_k^{uz}, a_k^{uz}, c\Delta t_k^u, c\Delta f_k^u]^T$$
$$\hat{\boldsymbol{X}}_k = [\hat{x}_k^u, \hat{v}_k^{ux}, \hat{a}_k^{ux}, \hat{y}_k^u, \hat{v}_k^{uy}, \hat{a}_k^{uy}, \hat{z}_k^u, \hat{v}_k^{uz}, \hat{a}_k^{uz}, c\Delta \hat{t}_k^u, c\Delta \hat{f}_k^u]^T$$
$$\hat{\boldsymbol{X}}_{k|k-1} = [\hat{x}_{k|k-1}^u, \hat{v}_{k|k-1}^{ux}, \hat{a}_{k|k-1}^{ux}, \hat{y}_{k|k-1}^u, \hat{v}_{k|k-1}^{uy}, \hat{a}_{k|k-1}^{uy}, \hat{z}_{k|k-1}^u, \hat{v}_{k|k-1}^{uz}, \hat{a}_{k|k-1}^{uz}, c\Delta \hat{t}_{k|k-1}^u, c\Delta \hat{f}_{k|k-1}^u]^T$$

Where $[x_k^u, y_k^u, z_k^u]$, $[v_k^{ux}, v_k^{uy}, v_k^{uz}]$, $[a_k^{ux}, a_k^{uy}, a_k^{uz}]$ are the receiver's position, velocity, acceleration in ECEF respectively; Δt_k^u and Δf_k^u are the receiver's clock error and clock drift separately; $\hat{\boldsymbol{X}}_k$ is the optimal estimation of filtering for $\boldsymbol{X}_k$; $\hat{\boldsymbol{X}}_{k|k-1}$ is the predictive state vector of $\boldsymbol{X}_k$.

The error covariance matrix P_k of $\hat{\boldsymbol{X}}_k$ is a matrix of 11×11.

The $\hat{\boldsymbol{X}}_0$ and P_0 for each algorithm can be shown in *Table 1*.

Table 1: The value of $\hat{\boldsymbol{X}}_0$ and P_0 for each algorithm

Algorithm	Value
ZEKF	$\hat{\boldsymbol{X}}_0 = \boldsymbol{0}$ $P_0 = diag[1/\varepsilon_p \ \ 1/\varepsilon_v \ \ 1/\varepsilon_a \ \ 1/\varepsilon_p \ \ 1/\varepsilon_v \ \ 1/\varepsilon_a \ \ 1/\varepsilon_p \ \ 1/\varepsilon_v \ \ 1/\varepsilon_a \ \ 1/\varepsilon_t \ \ 1/\varepsilon_f]$ [a]
CEKF	$\hat{\boldsymbol{X}}_0 = [6300000,0,0,550000,0,0,550000,0,0,0]$ $P_0 = diag[1/\varepsilon_p \ \ 1/\varepsilon_v \ \ 1/\varepsilon_a \ \ 1/\varepsilon_p \ \ 1/\varepsilon_v \ \ 1/\varepsilon_a \ \ 1/\varepsilon_p \ \ 1/\varepsilon_v \ \ 1/\varepsilon_a \ \ 1/\varepsilon_t \ \ 1/\varepsilon_f]$ [a]
DU-EKF	$\hat{\boldsymbol{X}}_0 = \boldsymbol{0}$ $P_0 = diag[1/\varepsilon_p \ \ 1/\varepsilon_v \ \ 1/\varepsilon_a \ \ 1/\varepsilon_p \ \ 1/\varepsilon_v \ \ 1/\varepsilon_a \ \ 1/\varepsilon_p \ \ 1/\varepsilon_v \ \ 1/\varepsilon_a \ \ 1/\varepsilon_t \ \ 1/\varepsilon_f]$ [a]

[a] $\varepsilon_p = 10^{-14}, \varepsilon_a = 0.01, \varepsilon_v = 10^{-3}, \varepsilon_t = \varepsilon_f = 10^{-5}$

[b] $[x_0^u, y_0^u, z_0^u]$, $[v_0^{ux}, v_0^{uy}, v_0^{uz}]$, Δt_0^u and Δf_0^u are calculated by ILS algorithm, $[a_0^{ux}, a_0^{uy}, a_0^{uy}] = \boldsymbol{0}$

2. $\Phi_{k|k-1}$ and Q_{k-1}

$$\Phi_{k|k-1} = \begin{bmatrix} \Phi_{k|k-1}^x & & & \\ & \Phi_{k|k-1}^y & & \\ & & \Phi_{k|k-1}^z & \\ & & & \Phi_{k|k-1}^c \end{bmatrix}$$

$$Q_{k-1} = \begin{bmatrix} 2\alpha_x\sigma_x^2 Q_{k-1}^x & & & \\ & 2\alpha_y\sigma_y^2 Q_{k-1}^y & & \\ & & 2\alpha_z\sigma_z^2 Q_{k-1}^z & \\ & & & Q_{k-1}^c \end{bmatrix}$$

Because the dynamic model is Singer model, $\Phi_{k|k-1}$ and Q_{k-1} are depicted as follows. The receiver's motion in X axis is taken as an example.

Journal of Theoretical and Applied Information Technology
31st March 2013. Vol. 49 No.3

ISSN: 1992-8645 www.jatit.org E-ISSN: 1817-3195

$$\Phi^x_{k|k\text{-}1}=\begin{bmatrix}1 & T & \frac{1}{\alpha_x^2}(-1+\alpha_x+e^{-\alpha_x T})\\ 0 & 1 & \frac{1}{\alpha_x}(1-e^{-\alpha_x T})\\ 0 & 0 & e^{-\alpha_x T}\end{bmatrix}\quad Q^x_{k\text{-}1}=\begin{bmatrix}q_{11} & q_{12} & q_{13}\\ q_{21} & q_{22} & q_{23}\\ q_{31} & q_{32} & q_{33}\end{bmatrix}$$

$$q_{11}=(1\text{-}e^{\text{-}2\alpha_x T}+2\alpha_x T+2\alpha_x^3T^3/3\text{-}2\alpha_x^2T^2\text{-}4\alpha_x Te^{\text{-}\alpha_x T})/2\alpha_x^5$$
$$q_{22}=(4e^{\text{-}\alpha_x T}\text{-}3\text{-}e^{\text{-}2\alpha_x T}+2\alpha_x T)/2\alpha_x^3$$
$$q_{33}=(1\text{-}2e^{\text{-}2\alpha_x T})/2\alpha_x$$
$$q_{12}=q_{21}=(e^{\text{-}2\alpha_x T}+1\text{-}2e^{\text{-}\alpha_x T}+2\alpha_x Te^{\text{-}\alpha_x T}\text{-}2\alpha_x T\ +\alpha_x^2T^2)/2\alpha_x^4$$
$$q_{13}=q_{31}=(1\text{-}e^{\text{-}2\alpha_x T}\text{-}2\alpha_x Te^{\text{-}\alpha_x T})/2\alpha_x^3$$
$$q_{23}=q_{32}=(1+e^{\text{-}2\alpha_x T}\text{-}2e^{\text{-}\alpha_x T})/2\alpha_x^2$$

$\Phi^y_{k|k\text{-}1}$ and $\Phi^z_{k|k\text{-}1}$ refer to $\Phi_{x|k+1}$. $Q^y_{k\text{-}1}$ and $Q^z_{k\text{-}1}$ refer to $Q^x_{k\text{-}1}$. α_x , α_y , α_z are the reciprocal of the maneuver time constant for each axis, $\alpha_x=\alpha_y=\alpha_z=10^6$. σ_x^2 , σ_y^2 , σ_z^2 are the variance of the target acceleration in X,Y,Z respectively. T=1s, σ_x^2=σ_y^2=σ_z^2=100 [9].

The clock model [7] with white noise input comes from a second-order Markov process, as follows:

$$\Phi^c_{k|k\text{-}1}=\begin{bmatrix}1 & T\\ 0 & 1\end{bmatrix}\qquad Q^c_{k\text{-}1}=\begin{bmatrix}q_c^{11} & q_c^{12}\\ q_c^{21} & q_c^{22}\end{bmatrix}$$

$$q_c^{11}=\frac{h_0}{2}T+2h_{\text{-}1}T^2+\frac{2}{3}\pi^2h_{\text{-}2}T^3$$
$$q_c^{12}=q_c^{21}=2h_{\text{-}1}T+\pi^2h_{\text{-}2}T^3$$
$$q_c^{22}=\frac{h_0}{2T}+2h_{\text{-}1}+\frac{8}{3}\pi^2h_{\text{-}2}T$$

The parameters $h_0=9.4\times10^{-20}$, $h_{\text{-}1}=1.8\times10^{-19}$, $h_{\text{-}2}=3.8\times10^{-21}$ correspond to values for a typical quartz standard.

3. H_k and O_k

H_k is linearized from $f_k(\boldsymbol{X}_k)$=$\left[R_k^1\ \cdots\ R_k^n\ D_k^1\ \cdots\ D_k^n\right]^T$. Where R_k^s and D_k^s is respectively the pseudorange Formula (9) and the Doppler shift Formula (10) [1] between a visible satellite and the receiver, $s=1,\cdots,n$ (n is the total number of visible satellites).

$$R_k^s=\sqrt{(X_k^s-x_k^u)^2+(Y_k^s-x_k^u)^2+(Z_k^s-z_k^u)^2}+c\cdot t_k^u \quad (9)$$

$$D_k^s=\frac{[(X_k^s-x_k^u)\cdot(V_k^{sx}-v_k^{ux})+(Y_k^s-y_k^u)\cdot(V_k^{sy}-v_k^{uy})+(Z_k^s-z_k^u)\cdot(V_k^{sz}-v_k^{uz})]}{\rho_k^s}+c\cdot f_k^u \quad (10)$$

In Formula (9) and Formula (10), $[X_k^s,Y_k^s,Z_k^s]$ and $[V_k^{sx},V_k^{sy},V_k^{sy}]$ are position and velocity vector of the sth visible satellite in ECEF, ρ_k^s is the actual range between the sth visible satellite and the receiver, ρ_k^s=$\sqrt{(X_k^s-x_k^u)^2+(Y_k^s-y_k^u)^2+(Z_k^s-z_k^u)^2}$.

$$H_k=\begin{bmatrix}h^1_{1x|k} & 0 & h^1_{1y|k} & 0 & h^1_{1z|k} & 0 & 1 & 0\\ \vdots & \vdots & \vdots & \vdots & \vdots & \vdots & \vdots & \vdots\\ h^1_{nx|k} & 0 & h^1_{ny|k} & 0 & h^1_{nz|k} & 0 & 1 & 0\\ h^2_{1x|k} & h^1_{1x|k} & h^2_{1y|k} & h^1_{1y|k} & h^2_{1y|k} & h^1_{1z|k} & 0 & 1\\ \vdots & \vdots & \vdots & \vdots & \vdots & \vdots & \vdots & \vdots\\ h^2_{nx|k} & h^1_{nx|k} & h^2_{ny|k} & h^1_{ny|k} & h^2_{nz|k} & h^1_{nz|k} & 0 & 1\end{bmatrix}$$

Elements from Line 1 to Line n of H_k is linearized from Formula (9) while from Line $n+1$ to Line $2n$ of H_k is linearized from Formula (10).

$$h^1_{sx|k}=\frac{\partial R_k^s}{\partial x_k^u}=\frac{\partial D_k^s}{\partial v_k^{ux}}=\frac{(\hat{x}^u_{k|k\text{-}1}-X_k^s)}{\rho^s_{k|k\text{-}1}}$$

$$h^2_{sx|k}=\frac{\partial D_k^s}{\partial x_k^u}=\frac{(\hat{v}^{ux}_{k|k\text{-}1}-V_k^{sx})(\rho^s_{k|k\text{-}1})^2-(\hat{x}^u_{k|k\text{-}1}-X_k^s)J^s_{k|k\text{-}1}}{(\rho^s_{k|k\text{-}1})^2}$$

$$\rho^s_{k|k\text{-}1}=\sqrt{(X_k^s-\hat{x}^u_{k|k\text{-}1})^2+(Y_k^s-\hat{y}^u_{k|k\text{-}1})^2+(Z_k^s-\hat{z}^u_{k|k\text{-}1})^2}$$

$$J_k^s=(X_k^s-\hat{x}^u_{k|k\text{-}1})\cdot(V_k^{sx}-\hat{v}^{ux}_{k|k\text{-}1})+(Y_k^s-\hat{y}^u_{k|k\text{-}1})\cdot(V_k^{sy}-\hat{v}^{uy}_{k|k\text{-}1})+(Z_k^s-\hat{z}^u_{k|k\text{-}1})\cdot(V_k^{sz}-\hat{v}^{uz}_{k|k\text{-}1})$$

where $h^1_{sy|k}$ and $h^1_{sz|k}$ refer to $h^1_{sx|k}$; $h^2_{sy|k}$ and $h^2_{sz|k}$ refer to $h^2_{sx|k}$.

The covariance matrix O_k of the observation noise vector is a matrix of $2n\times2n$, O_k=$diag\left[o_1\ \cdots\ o_1\ o_2\ \cdots\ o_2\right]$, o_1=64 , o_2=0.04 .

4. $\boldsymbol{Z}_k$ and $\Delta\boldsymbol{Z}_k$

$$\boldsymbol{Z}_k=\left[r_k^1\ \cdots\ r_k^n\ d_k^1\ \cdots\ d_k^n\right]^T$$

$$\Delta\boldsymbol{Z}_k=[(r_k^1-\hat{r}^1_{k|k\text{-}1}),\cdots,(r_k^n-\hat{r}^n_{k|k\text{-}1}),(d_k^1-\hat{d}^1_{k|k\text{-}1}),\cdots,(d_k^n-\hat{d}^n_{k|k\text{-}1})];$$

$$\hat{r}^s_{k|k\text{-}1}=\sqrt{(X_k^s-\hat{x}^u_{k|k\text{-}1})^2+(Y_k^s-\hat{x}^u_{k|k\text{-}1})^2+(Z_k^s-\hat{z}^u_{k|k\text{-}1})^2}+c\cdot\hat{t}^u_{k|k\text{-}1};$$

$$\hat{d}^s_{k|k\text{-}1}=\frac{[(X_k^s-\hat{x}^u_{k|k\text{-}1})\cdot(V_k^{sx}-\hat{v}^{ux}_{k|k\text{-}1})+(Y_k^s-\hat{y}^u_{k|k\text{-}1})\cdot(V_k^{sy}-\hat{v}^{uy}_{k|k\text{-}1})+(Z_k^s-z^u_{k|k\text{-}1})\cdot(V_k^{sz}-\hat{v}^{uz}_{k|k\text{-}1})]}{\rho^s_{k|k\text{-}1}}+c\cdot\hat{f}^u_{k|k\text{-}1}$$

Where r_k^s and d_k^s are the pseudorange and the Doppler shift of sth visible satellite respectively.

In the simulation, all of the four algorithms (ILS, ZEKF, CEKF and DU-EKF) are used for GPS point dynamic positioning and velocity measurement. The specific process of ILS algorithm can be seen at *Several Algorithms for GPS Pseudorange Absolute Positioning* [14]; the process of ZEKF algorithm and CEKF algorithm are shown in *Figure1*; the process of DU-EKF algorithm is

Journal of Theoretical and Applied Information Technology
31st March 2013. Vol. 49 No.3

ISSN: 1992-8645 www.jatit.org E-ISSN: 1817-3195

shown in *Figure 2*.

With respect to the result of each algorithm, the position and velocity error of X, Y and Z are respectively shown in *Table 2* and *Table 3*.

Table 2: Position error of each axis for different algorithms (m)

Axis	Algorithm	Mean value	Standard deviation	Root mean square
	ILS	-0.3041	8.9346	8.9397
X	CEKF	0.0213	1.4897	1.4898
	DU-EKF	-0.0269	1.3784	1.3786
	ILS	0.4654	5.0010	5.0226
Y	CEKF	-0.0427	0.8759	0.8769
	DU-EKF	-0.1841	0.7081	0.7316
	ILS	-0.0109	3.9734	3.9734
Z	CEKF	-0.4672	0.5392	0.7135
	DU-EKF	-0.0913	0.4778	0.4864

Table 3: Velocity error of each error for different algorithms (m/s)

Axis	Algorithm	Mean value	Standard deviation	Root mean square
	ILS	-0.0038	0.0407	0.0409
X	CEKF	-0.0071	0.0154	0.0170
	DU-EKF	0.0038	0.0129	0.0134
	ILS	0.0006	0.0259	0.0259
Y	CEKF	0.0031	0.0077	0.0083
	DU-EKF	-0.0012	0.0084	0.0084
	ILS	-0.0018	0.0184	0.0185
Z	CEKF	-0.0051	0.0073	0.0089
	DU-EKF	-0.0011	0.0070	0.0071

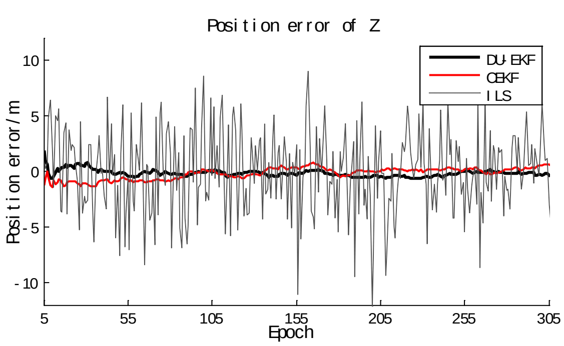

Figure 3: The position error of Z for different algorithms

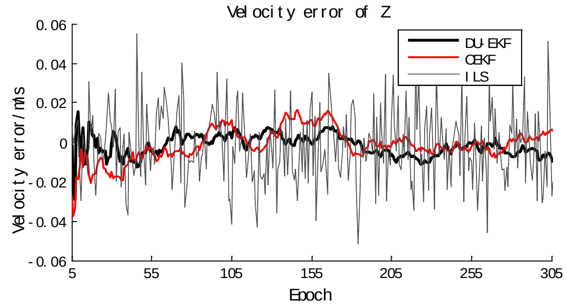

Figure 4: The velocity error of Z for diffeent algorithms

Figure 3 and *Figure 4* are the position error figure and velocity error figure of Z respectively. At the beginning 20 minutes of simulation for ZEKF algorithm, the position and velocity errors are much larger than other algorithms. So they are only shown in *Figure 5*. As shown in *Figure 3* and *Figure 4*, combining the statistic data in *Table 2* and *Table 3*, the position and velocity error of ILS algorithm are within 10*m* and 0.05*m/s* respectively; the position and velocity error of CEKF algorithm are within 2m and 0.02m/s respectively; the position error of DU-EKF algorithm are within 1.5m while the velocity error are within 0.02m/s. Compared with ILS algorithm, the precision of position and velocity of DU-EKF algorithm are much higher. Compared with CEKF algorithm, the precision of position and velocity of DU-EKF algorithm is not improved appreciably. But DU-EKF algorithm can accelerate the filter's convergence rate without the approximate value of the initial state vector.

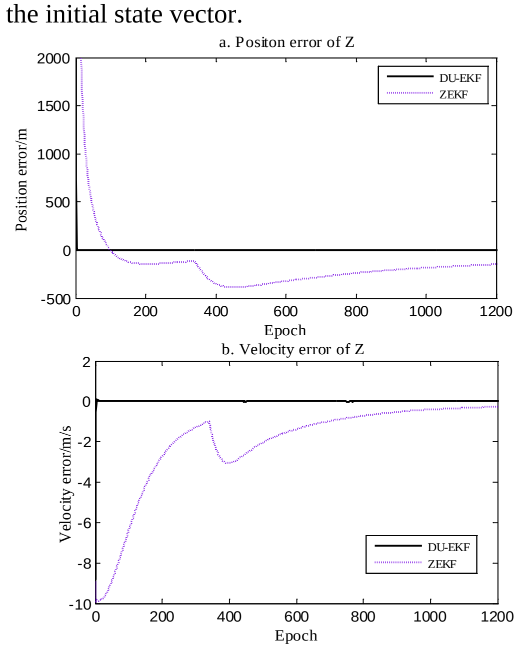

Figure 5: The error of Z for DU-EKF algorithm and ZEKF algorithm, a is the position error and b is velocity error

ISSN: 1992-8645 www.jatit.org E-ISSN: 1817-3195

As shown in *Figure 5*, when $\hat{X}_0$ is far from the actual X_0, the slow convergence of filter impedes dynamic positioning with extending the time of first positioning. *Figure* 5 demonstrates the effectiveness of DU-EKF algorithm in accelerating convergence rate of filter.

5. CONCLUSION

The example of uniform motion receiver is used in simulation of this study. By simulation, compared with ILS algorithm, CEKF algorithm and ZEKF algorithm, the effectiveness of the modified algorithm for EKF (DU-EKF algorithm) is demonstrated in GPS point dynamic positioning and velocity measurement. The results of DU-EKF algorithm have much higher precision than that of ILS algorithm and slightly higher accuracy than that of CEKF algorithm. DU-EKF algorithm solves the problem of low filter convergence rate without the initial approximate initial position of receiver (compared with ZEKF algorithm). DU-EKF algorithm sets the initial state vector as $\boldsymbol{0}$ which is far from the true value. However with the delayed updating of state error covariance matrix, the optimal estimation of filtering can be close to the actual state vector quickly.

If DU-EKF algorithm is used in actual GPS navigator, there is no need of receiver's initial approximate initial position all the time when it changes in a wide range. Meanwhile, higher precision of positioning and velocity measurement and less time consumption of first positioning can be reached. However, whether the DU-EKF algorithm can be applied in other areas or not should be further validated.

ACKNOWLEDGMENTS:

This work was supported by the National High-Tech. R&D Program, China (No.2011AA120505) and the National Natural Science Foundation, China (No.61173077).

REFRENCES:

[1] Bernhard Hofmann-Wellenhof et al, "GNSS global navigation satellite systems GPS, GLONASS, Galileo & more", Springer-Verlag, New York, 2008.

[2] Qing Chang et al, "GPS positioning algorithm based on least-square recurrence estimate", *Journal of Beijing University of Aeronautics and Astronautics*, Vol. 24, No. 3, 1998, pp. 263-266.

[3] Fred Daum, "Nonlinear filters: beyond the Kalman filter", *IEEE A&E SYSTEMS MAGAZINE*, Vol. 20, No. 8, 2005, pp. 57-69.

[4] Juang JC, Huang GS, "Application of Kalman filter and mean field annealing algorithms in GPS-based attitude determination", *Journal of navigation*, Vol. 51, No. 1, 1998, pp. 117-131.

[5] Gangyi Tu et al, "Implementation and validity of three GPS positioning optimization algorithms", *Journal of Chinese inertial technology*, Vol. 17, No. 2, 2009, pp. 170-174.

[6] Tong HB et al, "Iterative reweighted recursive least squares for robust positioning", *Electronics letters*, Vol. 48, No. 13, 2012, pp. 789-791.

[7] Xuchu Mao et al, "Nonlinear iterative algorithm for GPS positioning with bias model", *IEEE intelligent transportation systems conference*, October 3-6, 2004, pp. 684-689.

[8] Chui CK, Chen G, "Kalman filtering with real-time applications", 2nd ed, Springer-Verlag, New York, 1991.

[9] Robert A. Singer, "Estimating optimal tracking filter performance for manned maneuvering targets", *IEEE Transaction on aerospace and electronic systems*, Vol. AES-6, No. 4, 1970, pp. 473-483.

[10] Hampton RLT, James R. Cooke, "Unsupervised tracking of maneuvering Vehicle", *IEEE Transaction aerospace and electronic systems*, Vol. AES-9, No. 2, 1973, pp. 197-207.

[11] Moose RL, Vanlandingham HF, McCabe D.H., "Modeling and estimation for tracking maneuvering targets", *IEEE Transaction aerospace and electronic systems*, Vol. AES-15,No. 3, 1979,pp. 448-456.

[12] Pengfei Zhang et al. "Coordinate transformations in satellite navigation systems. Advances in electronic engineering, communication and management", *lecture notes in electrical engineering*, Vol. 140, 2012, pp. 249-257.

[13] Pengfei Zhang et al. "Time scales and time transformations among satellite navigation systems", *China satellite navigation conference (CSNC) 2012 proceedings*, lecture notes in Electrical Engineering, Vol. 160, Part 3, 2012, pp. 491-502.

[14] Qiuying Guo, Zhenqi Hu, "Several algorithms for GPS pseudorange absolute positioning", *Science of surveying and mapping*, Vol. 30,No. 5, 2005, pp. 26-28.